

Formation of Monolayer Graphene by Annealing Sacrificial Nickel Thin Films

A. J. Pollard,[†] R. R. Nair,[‡] S. N. Sabki,[†] C. R. Staddon,[†] L. M. A. Perdigo,[†] C. H. Hsu,[†]
J. M. Garfitt,[†] S. Gangopadhyay,[†] H. F. Gleeson,[‡] A. K. Geim,[‡] and P. H. Beton^{*,†}

School of Physics and Astronomy, University of Nottingham, Nottingham NG7 2RD, U.K., and School of Physics and Astronomy, University of Manchester, Schuster Laboratory, Brunswick Street, Manchester M13 9PL, U.K.

Received: June 29, 2009; Revised Manuscript Received: August 4, 2009

Graphene films have been formed by annealing Ni thin films at 800 °C under vacuum conditions. The Ni thin films are deposited on Si/SiO₂ and, following annealing, have a polycrystalline morphology with grain sizes on the order of 1 μm. Following growth, the Ni is removed by etching, and the graphene is transferred as a single continuous layer onto a separate surface. The fraction of monolayer graphene is investigated using optical and electron microscopy and Raman spectroscopy and is shown to be >75%.

Introduction

The isolation of individual atomic planes of graphite and the observation that the conductance of such monolayers can be controlled by a gate electrode has stimulated a new field of research into both the fundamental physics and the technological potential of graphene-related materials.^{1–4} In order to realize devices based on graphene, it is necessary to develop new methods for the controlled growth of mono- and few-layer graphitic films over large areas. There has been great progress in the growth of graphene on SiC,⁵ and an alternative methodology based on graphene suspensions formed by ultrasonic cleavage has also attracted considerable interest.⁶ It has also been shown that few-layer graphene can be grown on polycrystalline Ni substrates through exposure to methane at atmospheric pressure.^{7–10} Furthermore, the graphene can be released by etching the Ni substrate and then transferred to substrates better suited to technological applications, making this a very versatile approach to the formation of electrodes and active electronic components based on few-layer graphene. A similar approach using Cu films has recently been demonstrated to result in a high fraction of monolayer graphene.¹¹

For several technological applications, there is particular interest in the use of monolayer, rather than few-layer, graphene films due to their higher transconductance and optical transparency.¹² While the growth of few-layer graphene on Ni thin films has been reported relatively recently, the formation of monolayer graphene on single-crystal transition-metal substrates has been studied extensively in the surface science community.^{13–15} Due to the high cost and limited scalability of single-crystal metal substrates, it will be difficult to develop a viable process for technological applications based on this approach. Furthermore, graphene layers grown using this approach have not yet been isolated, and their electronic quality is untested. In a scalable variant of this procedure, it has recently been shown that monolayer graphene can be formed on Rh(111) thin films grown

epitaxially on Si(111) substrates which incorporate a buffer layer of yttria-stabilized zirconia.¹⁶ In this work, it was also demonstrated that graphene could be formed without the use of gaseous carbon-containing precursors and that the required carbon feedstock could be introduced by immersion of the sample in an organic solvent.

In this paper, we describe a route to the growth of graphene monolayers and their release and transfer to another substrate. In common with recent published work,^{7–9} polycrystalline Ni thin films are used as scalable sacrificial substrates. We find that annealing such samples, which are grown in a commercial thin film evaporator and passed through the atmosphere, results in the formation of graphene without the intentional introduction of an additional carbon source. We show that large areas of graphene, which are predominantly composed of a continuous monolayer, may be transferred to a dielectric substrate.

Experimental Methods

For substrates, we use Ni thin films deposited onto a 1 cm² piece of a Si(100) wafer with a SiO₂ layer of thickness 300 nm. The Ni layers have thicknesses in the range of 80–100 nm and are deposited by thermal sublimation in a standard commercial¹⁷ evaporator with a base pressure of ~10⁻⁶–10⁻⁷ mbar. The Ni thin films are then removed from vacuum and stored under atmospheric conditions for typical periods of a few days before being loaded into a separate vacuum system with a base pressure of ~5 × 10⁻¹⁰ mbar. The samples are initially outgassed by annealing at 500 °C (measured using a pyrometer) for ~12–18 h and are then annealed at temperatures ranging from 500–800 °C for 20 min. The samples are then allowed to cool to room temperature after reducing the current through a silicon strip heater to zero over a period of approximately 60 s. The samples are then extracted from the vacuum system and stored under ambient conditions.

Results and Discussion

The annealing cycles are critical for the formation of graphene films, with the best results obtained for temperatures in the range of 700–800 °C. Images acquired using an ambient atomic force

* To whom correspondence should be addressed. E-mail: peter.beton@nottingham.ac.uk. Tel: +44 115 9515129. Fax: +44 115 9515180.

[†] University of Nottingham.

[‡] University of Manchester.

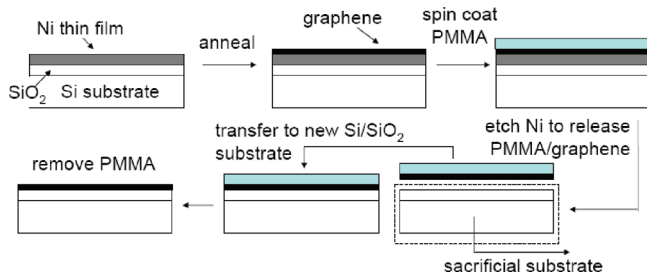


Figure 1. Schematic showing the process used to form graphene on Ni then transfer it^{7–9} to a separate substrate.

microscope (AFM) of samples following annealing are shown in Figure 2. The Ni grain size in the as-deposited films is ~ 20 – 30 nm, which increases as the film is annealed, with a significant change occurring for annealing temperatures between 700 and 800 °C, after which large (widths ~ 1 μm), highly faceted islands are observed. We have investigated these films using X-ray diffraction (results not shown), which shows peaks in a θ – 2θ scan consistent with the formation of (111)-oriented Ni crystallites.

The graphene layers are released from the Ni thin film by etching in a FeCl_3 solution (1 M)^{7–9} (see Figure 1). A polymethylmethacrylate (PMMA) thin film (250 nm) is spin-coated onto the sample in order to provide mechanical support and facilitate ease of handling. Following the release etch of the Ni layer, the PMMA/graphene layer is placed on a Si wafer on which a 90 nm thick SiO_2 layer has been grown or on a holey carbon grid used for electron microscopy. The PMMA layer is then dissolved by immersion in acetone. The oxide thickness is chosen to maximize the contrast in optical microscopy and allows the discrimination between mono- and few-layer graphene,¹⁸ as shown in Figure 2c and confirmed by electron microscopy (Figure 3) and Raman spectroscopy (Figure 4).

Figure 4 shows Raman spectra taken for areas of single- and few-layer graphene, as identified by optical microscopy. Spectra are measured with a $50\times$ objective at 514 nm excitation with a Renishaw micro-Raman spectrometer. A unique signature of single-layer graphene is a single Lorentzian peak at ~ 2690 cm^{-1} , which is often referred to as a 2D peak¹⁹ (in our case, with a full width at half-maximum (fwhm) of 33 cm^{-1}). For few-layer graphene, the peak normally develops into a broader 2D band.¹⁹ However, we find that in our films, the few-layer regions (the integrated G peak (~ 1590 cm^{-1}) intensity agrees well with a thickness of 3–4 layers consistent with optical microscopy (see Figure 4) still exhibit a single Lorentzian peak that however is much wider (FWHM of ~ 50 cm^{-1}). This is different from the behavior reported for micromechanically cleaved graphene and has previously been attributed to non-Bernal (turbostratic) stacking in the multilayer graphene films grown on Ni.⁸

These observations are confirmed using transmission electron microscopy. Diffraction patterns from single-layer regions (Figure 3b) have equally intense first- and second-order spots, consistent with single-layer graphene^{20,21} (the spot intensity is plotted in Figure 3d and should be compared with a similar dependence in ref 21), while multilayer regions give rise to multiple diffraction spots (Figure 3c) due to rotationally disordered (turbostratic) few-layer graphene.

A low-intensity D peak (disorder-induced) at 1350 cm^{-1} and a D' band at 1620 cm^{-1} are also observed in all single and few layers (Figure 4). This suggests defects or submicrometer cracks (we used a laser beam of ~ 2 μm in diameter), which are present within the continuous areas observed with optical microscopy.

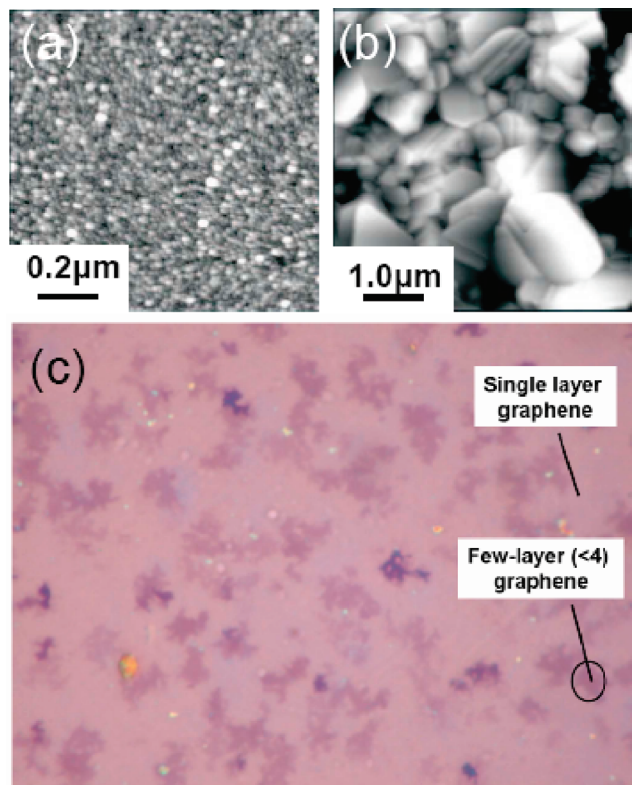


Figure 2. AFM images of (a) an as-grown Ni thin film, thickness 100 nm, and (b) that following vacuum annealing at 800 °C; (c) optical micrograph of graphene on a Si/SiO₂ substrate, showing contrast levels corresponding to monolayer and few-layer graphene. The horizontal field of view is 100 μm .

The presence of cracks is confirmed using scanning electron microscopy (Figure 3a), indicating that there are fewer defects in the graphene bulk than the intensity of the D peak suggests. Furthermore, the intensity of these defect-related peaks is smaller than that for graphene oxide, reduced graphene oxide,²² and graphane,²³ which indicates a good electronic quality of our films, but is still somewhat higher than that for the films reported in refs 8 and 9. From our images, we estimate (using an image histogram) that $\sim 75\%$ of the film is single-layer graphene and $\sim 25\%$ is few-layer (<4 layers). Only 1% of the area is covered with thicker films. Despite the simplicity of this approach, the proportion of the surface covered by monolayer, rather than few-layer, graphene is higher than the equivalent figure for growth on Ni using methane.^{7–9}

To determine the source of carbon, we have compared graphene derived from films grown in several different evaporators with minor variations in preparative procedures. Graphene which is similar to that discussed above is formed for films grown in evaporators with an oil-based primary (diffusion) or secondary (rotary) pump (the Edwards 306Auto¹⁷ has a turbomolecular pump backed by a rotary pump). We have also observed the formation of graphene in films grown in a system pumped by oil-free (turbomolecular, ion, and scroll) pumps. At this stage, it is not clear whether there is a single source of carbon contamination of the Ni films, but our observations suggest that carbon-containing compounds, for example, from background gases or adsorbates on the SiO_2 surface, can be incorporated into the Ni films during growth and subsequently converted to graphene during annealing.

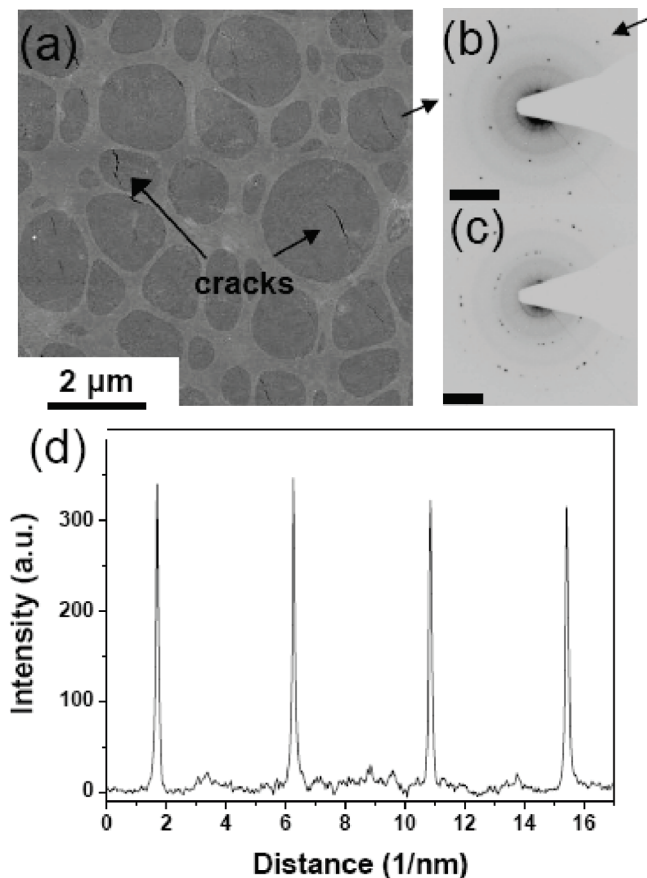


Figure 3. (a) SEM image of graphene transferred to a holey carbon TEM sample grid; dark gray regions are graphene, and cracks (black) can also be resolved; (b) and (c) TEM diffraction patterns (Tecnai F30, accelerating voltage 300 kV) from monolayer [(b) scale bar 4.3 nm⁻¹] and few-layer [(c) scale bar 3.8 nm⁻¹] regions; (d) intensity of diffraction spots versus position (in reciprocal space) along the line between the points marked by arrows in (b).

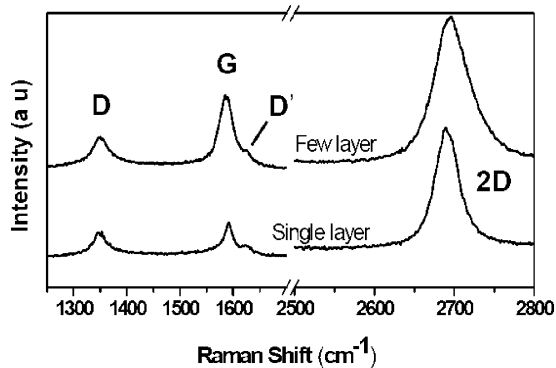


Figure 4. Raman spectrum of regions in Figure 2 identified as single-layer and few-layer graphene. Several peaks are identified and discussed in the text.

Conclusions

Overall, our results show that large-area graphene monolayers may be formed using the very simple process of annealing Ni

thin films in vacuum. This process converts trace amounts of unintentionally introduced carbon into graphene monolayers. Remarkably, this process is highly reproducible and results in films with a higher monolayer fraction than alternative approaches to graphene growth on nickel. Our results also highlight the potential importance of unintentional carbon sources, which must be considered when developing models for graphene growth.

Acknowledgment. This work was supported by the U.K. Engineering and Physical Sciences Research Council under Grant EP/C534158/1. We are grateful to Jasbinder Chauhan for technical assistance.

References and Notes

- (1) Novoselov, K. S.; Geim, A. K.; Morozov, S. V.; Jiang, D.; Zhang, Y.; Dubonos, S. V.; Grigorjeva, I. V.; Firsov, A. A. *Science* **2004**, *306*, 666.
- (2) Novoselov, K. S.; Geim, A. K.; Morozov, S. V.; Jaing, D.; Katsnelson, M. I.; Grigorjeva, I. V.; Dubonos, S. V.; Firsov, A. A. *Nature* **2005**, *438*, 197.
- (3) Zhang, Y. B.; Tan, Y. W.; Stormer, H. L.; Kim, P. *Nature* **2005**, *438*, 201.
- (4) Geim, A. K. *Science* **2009**, *324*, 1530.
- (5) Emstev, K. V.; et. al. *Nat. Mater.* **2009**, *8*, 203, and references therein.
- (6) Hernandez, Y.; et al. *Nat. Nano.* **2008**, *3* 563. Blake, P.; et al. *Nano Lett.* **2008**, *8*, 1704.
- (7) Yu, Q.; Lian, J.; Siriponglert, S.; Li, H.; Chen, Y. P.; Pei, S.-S. *Appl. Phys. Lett.* **2008**, *93*, 113103.
- (8) Reina, A.; Jia, X. T.; Nezich, J.; Son, H. B.; Bulovic, V.; Dresselhaus, M. S.; Kong, J. *Nano Lett.* **2009**, *9*, 3035.
- (9) Kim, K. S.; Zhao, Y.; Jang, H.; Lee, S. Y.; Kim, J. M.; Kim, K. S.; Ahn, J. H.; Kim, P.; Choi, J. Y.; Hong, B. H. *Nature* **2009**, *457*, 706.
- (10) Obraztsov, A. N.; Obraztsova, E. A.; Tyurnina, A. V.; Zolotukhin, A. A. *Carbon* **2007**, *45*, 2017.
- (11) Li, X.; Cai, W.; An, J.; Kim, S.; Nah, J.; Yang, D.; Piner, R.; Velamakanni, A.; Jung, I.; Tutuc, E.; Banerjee, S. K.; Colombo, L.; Ruoff, R. S. *Science* **2009**, *324*, 1312.
- (12) Nair, R. R.; Blake, P.; Grigorenko, A. N.; Novoselov, K. S.; Booth, T. J.; Stauber, T.; Peres, N. M. R.; Geim, A. K. *Science* **2008**, *320*, 180.
- (13) Eizenberg, M.; Blakely, J. M. *Surf. Sci.* **1970**, *82*, 228.
- (14) Sutter, P. W.; Flege, J.-I.; Sutter, E. A. *Nat. Mater.* **2008**, *7*, 406.
- (15) Coraux, J.; N'Diaye, A. T.; Busse, C.; Michely, T. *Nano Lett.* **2008**, *8*, 565.
- (16) Müller, F.; Sachdev, H.; Hufner, S.; Pollard, A. J.; Perkins, E. W.; Russell, J. C.; Beton, P. H.; Gsell, S.; Fischer, M.; Schreck, M.; Stritzker, B. *Small* **2009**, doi: 10.1002/smll.200900158
- (17) The evaporator used to deposit the Ni films was supplied commercially by Edwards, model Auto 306.
- (18) Blake, P.; Hill, E. W.; Neto, A. H. C.; Novoselov, K. S.; Jiang, D.; Yang, R.; Booth, T. J.; Geim, A. K. *Appl. Phys. Lett.* **2007**, *91*, 063124.
- (19) Ferrari, A. C.; Meyer, J. C.; Scardaci, V.; Gasiraghi, C.; Lazzeri, M.; Mauri, F.; Piscanec, S.; Jiang, D.; Novoselov, K. S.; Roth, S.; Geim, A. K. *Phys. Rev. Lett.* **2006**, *97*, 187401.
- (20) Meyer, J. C.; Geim, A. K.; Novoselov, K. S.; Booth, T. J.; Roth, S. *Nature* **2007**, *446*, 60.
- (21) Meyer, J. C.; Geim, A. K.; Katsnelson, M. I.; Novoselov, K. S.; Obergfell, D.; Roth, S.; Girit, C.; Zettl, A. *Solid State Commun.* **2007**, *143*, 101.
- (22) Gomez-Navarro, C.; Weitz, R. T.; Bittner, A. M.; Scolari, M.; Mews, A.; Burghard, M.; Kern, K. *Nano Lett.* **2007**, *7*, 3499.
- (23) Elias, D. C.; Nair, R. R.; Mohiuddin, T. M. G.; Morozov, S. V.; Blake, P.; Halsall, M. P.; Ferrari, A. C.; Boukhalov, D. W.; Katsnelson, M. I.; Geim, A. K.; Novoselov, K. S. *Science* **2009**, *323*, 610.